Curve fit estimate of roll damping for high damping cases

Timothy Smith, *Naval Surface Warfare Center Carderock Division,* timothy.c.smith1@navy.mil

ABSTRACT

Free decay roll damping experiments at forward speed are more difficult to perform than at zero speed. The resulting roll time history often has more noise and fewer peaks to analyze to determine the roll damping. As a result, conventional roll damping analysis methods based on successive peaks produces just a few data points per run with high uncertainty. A curve fitting approach to data analysis is demonstrated for the analysis of highly damped free roll decay experiments.

Keywords: *roll damping, digital filtering.*

1. INTRODUCTION

Zero speed roll decay tests can be performed with a high degree of precision and control of initial conditions (Katayama et al., 2018; Oliva-Remoal et al., 2018; Sumislawski et al., 2018). Due to relatively low damping, often between 5-15% of critical damping, many oscillations exist to analyze and determine the roll damping. With forward speed, the roll damping increases due to hull and appendage lift. This is not necessarily a problem for forced rolling experiments where the model is excited by moving weights or gyroscopes. The roll damping analysis of forced rolling experiments does not depend on decreasing peaks. However, for free roll decay experiments, the increased damping results in fewer peaks to analyze requiring more data to define the roll damping behavior. Also, exciting the model to an initial roll angle with an external stimulus is difficult with a moving target.

Park et al. (2009, 2016, 2017) and Smith (2018) have both presented curve fitting approaches to roll decay analysis that would be appropriate for higher damping cases. Park et al. fits a decaying sine function to the entire time history to determine the roll damping coefficient and natural roll frequency. This is a linearization of the roll damping. Analysis of many time histories with varying initial conditions and model speed determines the dependency on roll angle and speed. Smith (2018) follows a similar approach but curve fits the decaying sine function to each cycle or oscillation. This produces more data points per run; the same number of points per run as peak-based analysis.

Though not often performed, pitch damping experiments are also instances of highly damped oscillations. Often only a single oscillation occurs for conventional monohulls. Figure 1 is an example of a pitch decay after a sensor polarity check. The conventional peak based analysis is not necessarily possible. A curve-fitting approach is an attractive alternative.

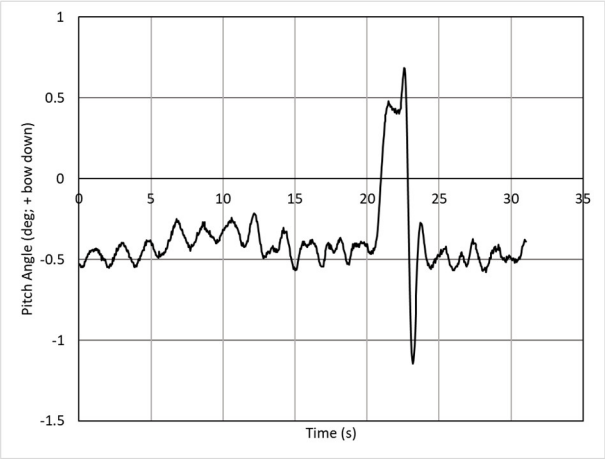

Figure 1: Example pitch decay with model held bow down and released.

A curve fitting approach will be demonstrated with simulated and actual time histories for highly damped conditions. The amount of data required for the curve fit is investigated. The use of a different curve fit function is shown for over damped cases.

2. NONLINEAR ROLL EQUATION

Synthetic data with noise was generated with a single degree-of-freedom differential equation having quadratic damping and cubic restoring (Smith, 2018; Vassilopoulos, 1971, Dalzell, 1978).

The single degree of freedom linear roll equation is a simple harmonic oscillator; Equation (1).

$$(I_{44} + A_{44})\ddot{\varphi} + B_{44\_l}\dot{\varphi} + C_{44}\varphi = 0 \quad (1)$$

$$C_{44} = GMg\Delta \quad (2)$$

where I_{44} is the roll mass moment of inertia, A_{44} is the roll added mass, B_{44_l} is linear roll damping, and C_{44} is linear hydrostatic stiffness, GM is the metacentric height, g is the acceleration due to gravity, and Δ is the ship displacement.

Re-writing Equation 1 in standard form results in Equation 3 (Karnopp, 1974)

$$\ddot{\varphi} + 2\zeta\omega_n\dot{\varphi} + \omega_n^2\varphi = 0 \quad (3)$$

$$\omega_n = \sqrt{C_{44}/(I_{44} + A_{44})} \quad (4)$$

$$\zeta = B_{44\_l}/2\sqrt{C_{44}(I_{44} + A_{44})} \quad (5)$$

where ω_n is the undamped natural frequency and ζ is the damping ratio.

The free decay solution of which is given in Equation (6):

$$\varphi = e^{-\omega_n\zeta t}\left(\frac{v_o + \omega_n\zeta x_o}{\omega_n\sqrt{1-\zeta^2}}\sin\omega_n\sqrt{1-\zeta^2}t + x_o\cos\omega_n\sqrt{1-\zeta^2}\,t\right) \quad (6)$$

where x_o and v_o are initial heel angle and roll velocity, respectively. The solution can also be written as a damped sine wave:

$$\varphi = e^{-\omega_n\zeta t}\sin\left(\omega_n\sqrt{1-\zeta^2}t + \varepsilon\right) \quad (7)$$

where ε is the phase angle set to match initial heel angle and roll rate. Equations (6) and (7) assume a zero mean heel angle. A non-zero mean heel angle. $\varphi_{OM,}$ can easily be added as seen in Equation (8).

$$\varphi = \varphi_o + e^{-\omega_n\zeta t}\,x_o\sin\left(\omega_n\sqrt{1-\zeta^2}t + \varepsilon\right) \quad (8)$$

Adding nonlinear damping and nonlinear stiffness in a single degree of freedom equation gives:

$$\ddot{\varphi} + 2\zeta\omega_n\dot{\varphi} + \beta\dot{\varphi}|\dot{\varphi}| + \omega_n^2\varphi + \gamma\varphi^3 = 0 \quad (9)$$

where the damping value is dependent on roll angle and forward speed and the stiffness values represent the righting arm curve. β is the normalized quadratic damping and γ is the normalized cubic stiffness terms. Equation 9 was solved with a fourth order Runge-Kutta method to provide roll decay data with known properties.

Experimental data from a free decay experiment will often have noise overlaid on the free decay caused by impulsive loading, steering, wave reflection, static heel, sensor error. To approximate that noise,φ_N, a sine wave (Equation (10)) was overlaid on the numerical solution to Equation (9). A sine wave was selected rather than white noise as experience indicates signal noise is due to cross-coupling from impulsive loading and steering.

$$\varphi_N = \varphi_{o_N} + \varphi_{A_N}(t_N - t)\sin(\omega_N t + \varepsilon_N)/t_N \quad (10)$$

The parameters for Equation (9) and the noise sine wave,φ_{o_N}, φ_{A_N} and ω_N, are set to nominal values as shown in Table 1. The Equation (9) parameters are typical monohull damping values with a roll period of 10.25 s. An initial roll angle of 30 degrees was selected to provide a number of peaks in a single time history. The noise sine wave parameters were selected to provide roughly 5% error that varied over the time history. The slower frequency, ω_N, represents a rudder steering or yaw influence. The parameters of the sine wave,φ_{o_N}, φ_{A_N} and ω_N, are set to nominal values as shown in Table 1. The noise ramp length, t_N, was set to the time the roll angle became small (approximately 0.2 deg). The phase, ε_N, was randomly selected.

Table 1. Coefficients for roll ordinary differential equation (Equation 9) and noise (Equation 10).

Coefficient	Units	Value
ω_n	rad/s	0.613
ζ		0.25/0.60
β		0.200
γ		0.00
x_o	deg	30.00
v^o	deg/s	0.00
φ_{o_N}	deg	0.00
φ_{A_N}	deg	3.0 (10%)
$_N$	rad/s	0.200
t_N	s	20/40

3. CURVE FITTING PROCESS

Free decay time histories can be analyzed with a number of approaches from various successive peak ratios assuming a logarithmic decrement (Handschel et al., 2015), energy loss (Handschel et al., 2015) or curve fitting techniques (Park et al., 2017). Smith (2018) demonstrated these methods produce the same results for noise free data.

The time history data were fitted with a damped sine wave (Equation (7)) over various amounts of data; half cycles, full cycles, and from each peak to the end of the run (referred to as "All"). The "All" fit damping values are associated with the initial data peak value following Park et al. (2009). Fitting the entire run linearizes the results but provides a more stable answer as more data are employed when curve fitting. Fitting smaller amounts of data captures the roll angle dependence with a potential loss of accuracy.

With curve fitting a damped sine wave, the natural frequency can be estimated as well as the damping ratio, ζ. Peak analysis of the time history will result in the damped natural frequency. This must be converted to the natural frequency by dividing the damped natural frequency by $\sqrt{1-\zeta^2}$.

The curve fitting was done with Microsoft Excel Solver function minimizing the sum of the square of the differences in time histories. Solver did not find a good answer in some instances and needed to be re-run with a better initial guess.

4. EXAMPLES

Increasing the damping reduces not only the size of the oscillation but the number of oscillations and frequency of oscillation as shown in Figure 2. Damping values above 0.5 tend to look quite similar and experimentally are nearly indistinguishable from critically and over damped cases. Bishop et al. (2005) indicates forward speed roll damping values between 0.15 – 0.25.

Two synthetic roll time histories was generated with a linear damping coefficient (0.25 and 0.60) and a quadratic damping coefficient of 0.20. A sine wave representing noise from Equation (10) was overlaid on the roll time history. The noise amplitude employed a 40 second ramp. In Figures 3 – 7, the "Theory" line is the known solution; the "Data Fit" is the fit considering all data except those obviously corrupted by noise. This was determined by looking for a change in trend or increase of scatter or non-sensical values, such as negative damping.

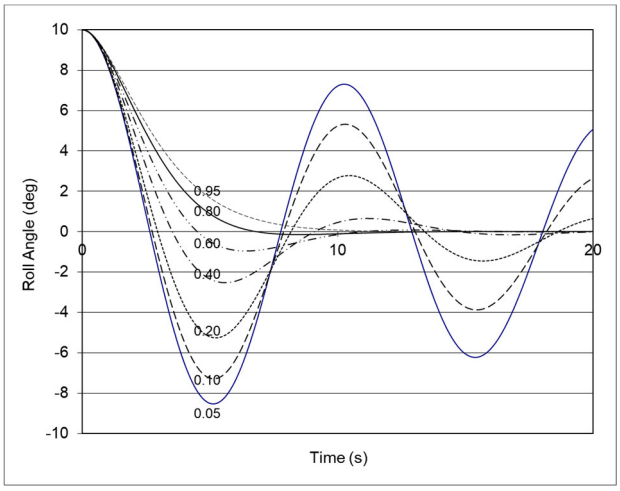

Figure 2: Roll decay curves with different linear damping coefficients ranging from 0.05 to 0.95.

Synthetic data ζ=0.25

A roll time history was generated with a linear damping coefficient of 0.25. The noise amplitude employed a 40 second ramp. The damping ratio (fraction of critical damping) for the different curve fitting approaches is shown in Figure 3.

In this case, all of the approaches, half, full, or all, would have provided a reasonable estimate of the roll damping. However, the use of data from all three approaches enables a better recognition of the damping trend with respect to roll angle. The linear regression of the data results in line nearly the same as the theoretical value.

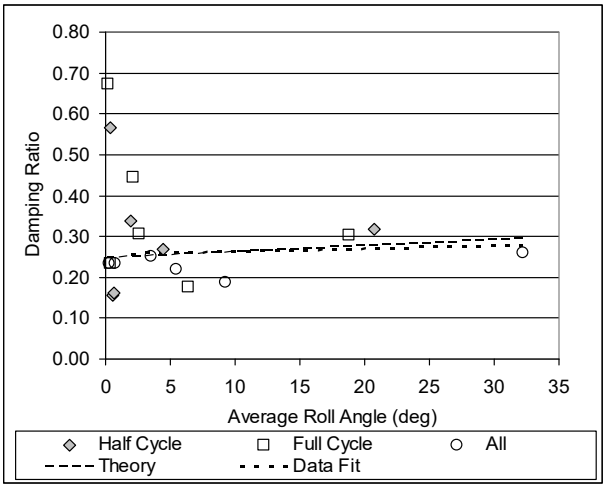

Figure 3: Roll damping ratio from time history curve fitting for synthetic data with linear damping of 0.25.

Synthetic data ζ=0.6

A roll time history was generated with a linear damping coefficient of 0.60. The noise amplitude employed a 20 second ramp. The damping ratio (fraction of critical damping) for the different curve fitting approaches is shown in Figure 4.

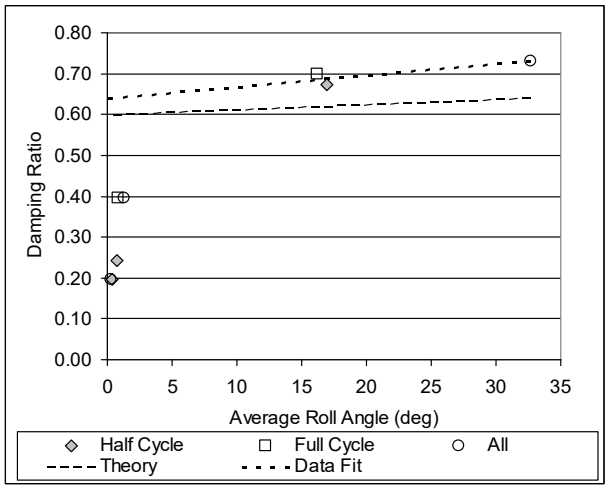

Figure 4: Roll damping ratio from time history curve fitting for synthetic data with linear damping of 0.6.

This example again shows the benefit from multiple curve fitting approaches to generate more data and identify trends. A single approach would result in either a single usable data point or an incorrect roll damping estimate with small linear damping and large quadratic damping.

Experimental data ζ=0.153

Free roll decay data from Bishop et al. (2005), Flare Topside at 25 knots (run 341) was analyzed with the curve fitting approach. This run has two impulses and decays. The decays were analyzed with a full cycle logarithmic decrement approach. The time histories were analyzed with a curve fitting method. Figure 5 is a comparison of curve fit results to reported results.

A number of curve fits did not result in acceptable results on the first attempt. Fixing the initial amplitude helped some instances but generally increased the data scatter. This type of difficulty usually indicates the presence of noise. Examination of the peaks indicated they were not monotonically decreasing. In this case, data fits with more data may have more error as more noisy cycles are included.

Bishop et al. results are very similar to the Full cycle curve fitting results. The data has the typical noise at low roll angles which are usually ignored but are included here for completeness. The trends at the highest roll angles have a notable difference between the Half cycle, Full cycle, and All data points. The "Data Fit" line employed the Half cycle points rather than All as the All values are less than both the Half and Full data. The resulting "Data Fit" line falls along Bishop et al. and Full cycle data. Inclusion of All data and not Half data resulted in a nearly horizontal "Data Fit" line. Use of only the Half cycle data would result in a slightly steeper data fit.

Whether or not curve fitting provided a significant advantage over the logarithmic decrement approach based on peaks is unclear.

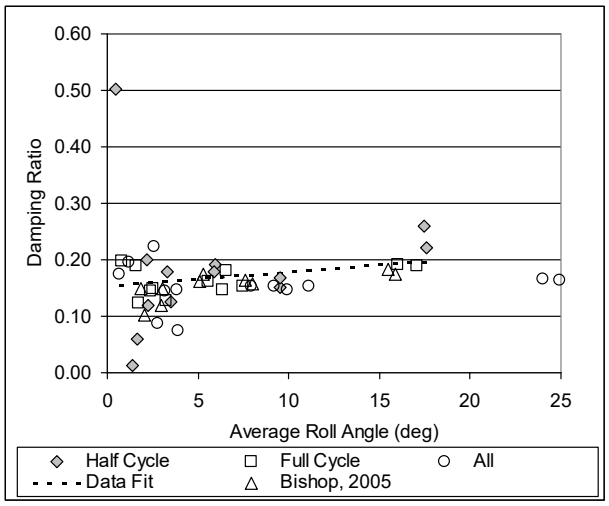

Figure 5: Roll damping ratio from ONR flare-topside time history at 25 knots (run 341).

Experimental data ζ=0.305

A more heavily damped experimental free roll decay run with a single-oscillation decay was analyzed with curve fitting. The run had two impulses and decays as shown in Figure 6. The speed was 19.2 knots full-scale. As a point of interest, pitch decay experiments have similar behavior as shown in Figure 1.

Figure 7 shows the roll damping ratio from the curve fitting analysis. Peak-based logarithmic decrement analysis had damping values from 0.53 to 0.68 with comparable data scatter. From the number of oscillations, Figure 2 indicates a damping value should be between 0.4 and 0.6. The curve fitting approach has better correlation to expected values.

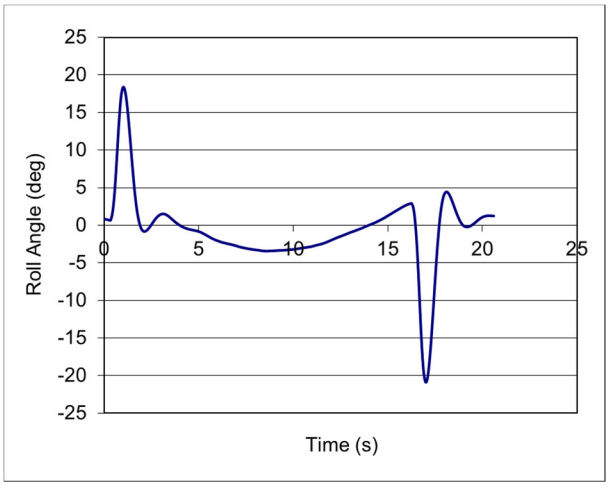

Figure 6: Time history data for single oscillation decay.

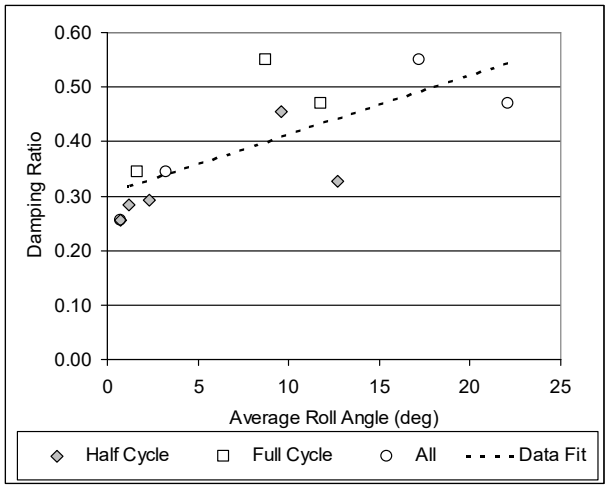

Figure 7: Roll damping ratio from experimental data with one oscillation.

Digital filtering

The noise in the roll data due to other couple motions does affect the accuracy of the estimated roll damping value. Shifting the data with an offset to correct a non-zero mean value is recommended and commonly done (Smith, 2018; Handschel et al., 2015). Further noise removal was attempted with digital filtering based on the premise that by eliminating frequencies not near the roll frequency would remove the noise allowing the data to be analyzed more accurately. This approach worked well with synthetic data where a second low frequency oscillation was added to the roll decay time history. The two peaks were easily identified after Fast Fourier Transform (FTT) and the noise peak can be removed.

With experimental data, the roll peak can be easily identified, but a noise peak may not be apparent. However, looking at ONR Flare Topside run 341 with 512-point FFT, two peaks were found as shown in Figure 8. The roll frequency from the damping analysis was 3.49 rad/s; this corresponds to the higher frequency peak. Time histories of the roll and noise signal were calculated by an inverse FFT of the spectrum filtered with a notch filter as shown in Figure 9.

Some noise is expected based on the damping analysis. The amplitude of the noise time history was larger than expected. Removal of the noise reduces the first amplitude about 40%. Roll damping values would be much different between the measured and "no noise" roll time histories. Without a benchmark value for comparison, determining if too much "noise" has been removed is difficult. Nevertheless, with more study digital filtering could possibly improve roll damping estimates.

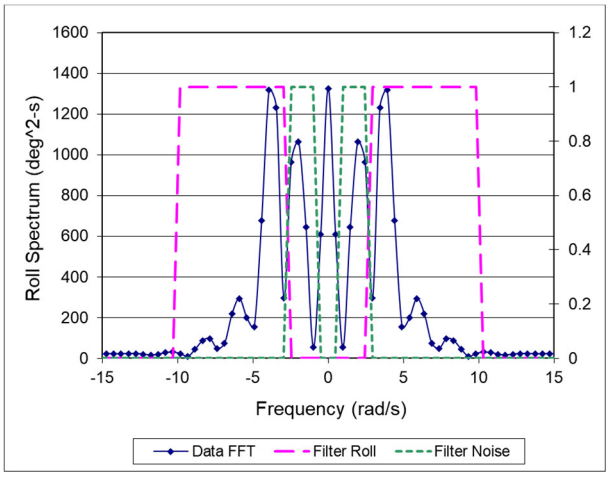

Figure 8: Roll spectrum of ONR Flare-Topside run 341 with notch filter.

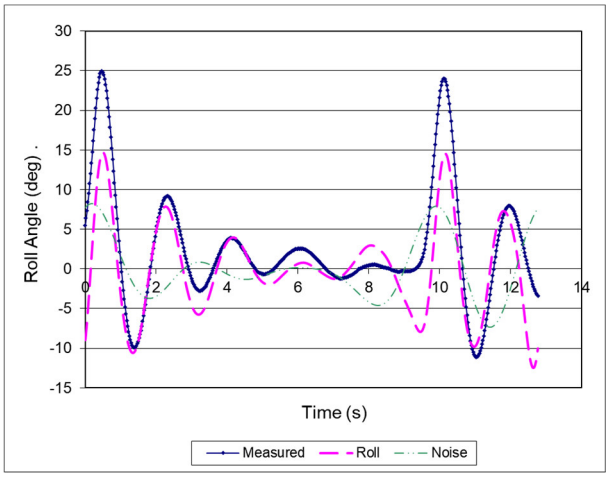

Figure 9: Time histories of ONR Flare-Topside run 341 as measured and decomposed to roll and noise signal.

5. OVERDAMPED CASES

Time histories without an oscillation by definition have damping coefficients greater than or equal to 1. In practice, time histories with damping coefficients greater than approximately 0.7 can also appear to not be oscillatory and be considered critically damped (Lloyd, 1989). However, the solution to roll motion ODE changes for critically damped and over damped cases. From Karnopp (1974), the overdamped solution is:

$$\varphi = e^{-\omega_n \zeta t}\left(\frac{v_o + \omega_n \zeta x_o}{\omega_n\sqrt{\zeta^2 - 1}}\sinh \omega_n\sqrt{\zeta^2 - 1}t + x_o \cosh \omega_n\sqrt{\zeta^2 - 1}\,t\right) \quad (11)$$

The case of critical damping has another solution. In practice, real systems are either under or over damped, rather than exactly critically damped.

Any curve fitting with a damped sine wave may not produce a result or produce an incorrect result in the over damped cases. The curve fitting process will match a portion of an oscillatory curve with the overdamped experimental data. In these cases, specifying the initial roll angle and roll rate rather than allow the curve fitting algorithm to find a match for them is necessary.

6. CONCLUSIONS

A damped sine wave was fit to roll decay data to determine the damping ratio and natural frequency. Different durations of data from Half cycle, Full cycle, and peak to end (All) were applied to the curve fit to determine the dependency on roll angle and amount of data. The use of all three was helpful to determine trends respect to roll angle. Curve fitting was especially useful for cases with very few oscillations. However, curve fitting did not necessarily produce a unique solution and multiple curve fitting attempts with different initial guess may be needed.

Digital filtering as a noise removal method shows potential. More study and benchmarking is needed to determine a robust filter.

Curve fitting of over damped cases should be possible with the solution to the over damped oscillator. Sensitivity to initial guess for the optimization algorithm may be larger than seen with the under damped cases.

7. ACKNOWLEDGEMENT

This work was supported by Dr. Woei-Min Lin of Office of Naval Research.

REFERENCES

Bassler, C. C., Reed, A. M. and Brown, A. J., 2010, "Characterization of Energy Dissipation Phenomena for Large Amplitude Ship Roll Motions", Proceedings of the 29th American Towing Tank Conference, Annapolis, MD, USA.

Bishop, R., Belknap, W. , Turner, C., Simon, B., and Kim, J. H., 2005, "Parametric Investigation on the Influence of GM, Roll damping, and Above-Water Form on the Roll Response of Model 5613", Report NSWCCD-50-TR-2005/027.

Dalzell, J. F., 1978, "A Note on the Form of Ship Roll Damping," Journal of Ship Research, Vol 22, No. 3, Sep 1978, pp. 178-185

Handschel. S., Fröhlich, M., and Abdel-Maksoud, M., 2014, "Experimental and Numerical Investigation of Ship Roll Damping by Applying the Harmonic Forced Roll Motion Technique", 30th Symposium on Naval Hydrodynamics, Hobart, Tasmania, Australia.

Handschel, S., Feder, D., and Abdel-Maksoud, M., 2015, "Estimation of Ship Roll Damping – A Comparison of the Decay and the Harmonic Excited Roll Motion Technique for a Post Panamax Container", Proc. 12th Intl. Conf. on the Stability of Ships and Ocean Vehicles, Glasgow, UK, 19-24 June, page 475-488.

Hashimoto, H., Omura, T., Matsuda, A., Yoneda, S., Stern, F., and Tahara, Y., 2018, "Some Remarks on EFD and CDF for Ship Roll Decay", Proceedings of the 10th International Conference on Stability of Ships and Ocean Vehicles, (STAB2018), Kobe, Japan, pp. 339-348

Karnopp, B., 1974, Introduction to Dynamics, Addison-Wesley, pp. 291-296.

Katayama, T., Adachi, T., Sawae, T., 2018, "Roll Damping Estimation for Small Planing Craft", Proceedings of the 10th International Conference on Stability of Ships and Ocean Vehicles, (STAB2018), Kobe, Japan, pp. 369-378.

Llyod, A. R. J. M., 1989, Seakeeping – Ship Behaviour in Rough Weather, Ellis Hornwood.

Oliva-Remola, A., Perez-Rojas, L., Diaz-Ojeda, H., 2018, "Ship Roll Damping Estimation: A Comparative Study of Different Roll Decay Tests," Proceedings of the 10th International Conference on Stability of Ships and Ocean Vehicles, (STAB2018), Kobe, Japan, pp. 312--322.

Park, J. T., Hayden, D. D., Klamo, J., and Bishop, R. C., 2009, "Analysis Methodology of Roll Decay Data for Free-Running and Captive Model Tests", Proceedings of the 18th International Conference of Ship and Shipping Research, Vol. 1, pp. 105-114, Messina, Italy.

Park, J. T., Turner, C. R., and Melendez, M. P., 2016, "Physical Properties and Roll Decay with Uncertainty Estimates for DTMB Model 5720, 23rd Scale R/V Melville", NSWCCD-80-TR-2016/018.

Park, J. T., Turner, C. R., and Melendez, M. P., 2017, "New Methodology in Analysis of Physical Properties and Roll Decay with Uncertainty Estimates for Surface-Ship Model Experiments", Proceedings 30th American Towing Tank Conference, West Bethesda, USA, 3-5 October, 2017.

Smith, T., 2018, "Determination of Roll Damping for Empirical Measurements", Proceedings of the 10th International Conference on Stability of Ships and Ocean Vehicles, (STAB2018), Kobe, Japan, pp. 301-311.

Sumislawski, P., Wassermann, S. Abdel-Maksoud, M., 2018, "Rudder Influence on Roll Damping", Proceedings of the 10th International Conference on Stability of Ships and Ocean Vehicles, (STAB2018), Kobe, Japan, pp. 360-368.

Vassilopoulos, L., 1971, "Ship Rolling at Zero Speed in Random Beam Seas with Nonlinear Damping and Restoration", Journal of Ship Research, Vol. 15, No. 4.